Estimation of sheath electric field in inductively coupled hydrogen plasma on the basis of Doppler-broadened absorption spectrum of hydrogen Balmer-α line

Shusuke Nishiyama[1], Kosuke Takada[2], and Koichi Sasaki[2*]

[1] *Faculty of Health Science, Japan Healthcare University, 1-50, 11-choume, Tsukisamu-Higashi 3-jo, Toyohira-ku, Sapporo, 062-0053, Japan*

[2] *Division of Applied Quantum Science and Engineering, Hokkaido University, Kita 13, Nishi 8, Kita-ku, Sapporo 060-8628, Japan*

We examined the applicability of the Doppler-broadened absorption spectrum of the hydrogen Balmer-α line to the estimation of the sheath electric field in plasma. The Stark splitting of the fine-structure components was calculated by solving the time-independent Schrödinger equation at various electric field strengths, and the theoretical absorption spectrum was obtained by the superposition of the fine-structure components with the same Doppler broadening widths. The spectrum of the Balmer-α line of atomic hydrogen, which was measured by standard diode laser absorption spectroscopy, was fitted with the theoretical spectrum. We succeeded in determining the translational temperature of atomic hydrogen, which was obtained from the Doppler broadening width, and the electric field strength by the spectral fitting. We have evaluated that the minimum electric field strength that can be detected by the present method is approximately 350 V/cm when the translational temperature of atomic hydrogen is 400-500 K.

1. Introduction

The electric field in a sheath, which is formed between a plasma and a solid surface, is an old and new problem in plasma physics.[1,2] The sheath electric field in unmagnetized plasma can be predicted on the basis of the standard Bohm theory,[3] if the plasma is electropositive, the collision in the sheath is negligible, the sheath is static, and the plasma has a single ion species. However, the structures of the sheath electric fields in actual plasmas are deviated from ideal ones. Although many works have been carried out, we have not reached the perfect understanding of the electric field structures in collisional sheaths,[4–8] electronegative sheaths,[9–13] and sheaths with multiple ion species.[14–16] In addition, the transition region between the ion sheath and the presheath has been discussed intensively.[17–23]

A difficulty in the study of the sheath electric field is caused by the lack of an easy-to-use

*Corresponding author, E-mail: sasaki@qe.eng.hokudai.ac.jp

method that is applicable to experiments. Since an emissive probe has an insufficient spatial resolution and causes considerable disturbance to the sheath, a non-contact method with a fine spatial resolution is demanded. The representative non-contact method, which can be used in low-pressure plasmas, is laser Stark spectroscopy. The Stark effect is the change in the energy level structure of an atom or a molecule in electric field. The energy of an excited state or the wavelength of a transition line is a function of the electric field, and we can determine the electric field by measuring the spectrum of an optical transition line. In principle, the electric field measurement by Stark spectroscopy have no limitation in electron density and electron temperature. It is noted here that a higher energy state (a Rydberg state) shows more sensitive response to weak electric field. Hence, the conventional trend in laser Stark spectroscopy for the sensitive sheath electric field measurement was the development of a method for detecting high Rydberg states.[24–34] However, the trend toward high Rydberg states stands in the trade-off relationship with the decrease in the detection sensitivity, since the transition probability decreases steeply with the principal quantum number.

In a previous work, we changed our approach to lower-lying energy states.[35,36] Although lower-lying states show less sensitive Stark effect, they can be detected rather easily by laser absorption spectroscopy. We compensated the less sensitive Stark effect by employing saturated absorption spectroscopy with a Doppler-free wavelength resolution. We have succeeded in detecting weak electric field of $\sim$ 10 V/cm in the sheath by employing the Balmer-α line of atomic hydrogen.[36] This sensitivity is comparable to that realized by laser-induced fluorescence-dip spectroscopy,[28–34] where Rydberg states with principal quantum numbers up to $n = 40 - 55$ are detected. However, the Stark spectroscopy of lower-lying states combined with saturated absorption spectroscopy is problematic in strong electric field ($\geq$ 500 V/cm). One problem is the crossover resonances which appear at the center between two transition lines with common lower or upper energy states. The Balmer-α line of atomic hydrogen splits into many fine structure components in the strong electric field, and in this case the saturated absorption spectrum becomes complicated because of many crossover peaks. Another problem is the decrease in the depth of the Lamb dip, which is due to the small transition probability of the line with the Stark splitting.

In this work, we examined the applicability of Doppler-broadened absorption spectrum of the hydrogen Balmer-α line to the measurement of the sheath electric field. The wavelength resolution of standard laser absorption spectroscopy employing a tunable single-mode laser is limited by the Doppler broadening, and it is much worse than that of saturated absorption spectroscopy. However, it would be possible to utilize the Doppler-broadened absorption

spectrum for the estimation of relatively strong electric field. The applicability of the Doppler-broadened spectrum of the Balmer-α and Balmer-β lines of atomic hydrogen to the electric field measurement was investigated by several authors.[37–42] Since the spectroscopic methods used in their experiments were optical emission spectroscopy with limited wavelength resolutions, the detection limits achieved in these experiments were on the order of kV/cm even when the Balmer-β line was employed. In this work, we employed laser absorption spectroscopy, which has a better wavelength resolution than optical emission spectroscopy, for the measurement of the spectrum of the Balmer-α line. We have evaluated the minimum electric field that can be determined on the basis of the Doppler-broadened absorption spectrum.

2. Principles and theoretical absorption spectra

Figure 1 shows the energy level diagram of atomic hydrogen relevant to the Balmer-α line. The Balmer-α line is the transition between energy levels with principal quantum numbers of $n = 2$ and 3. Because of the fine structures and the selection rule, the Balmer-α line is composed of seven transition lines in the field-free condition. An example of the theoretical absorption spectrum of the field-free Balmer-α line is shown in Fig. 2(a). In this spectrum, we assume that the ratio of the population densities of the three $n = 2$ states, including the metastable $2s^2S_{1/2}$, is given by the statistical weights. The population distribution which is equal to the statistical weights is widely observed in literature.[43–47] It is realized by the large rate coefficient of $H(2s^2S_{1/2}) + e \rightarrow H(2p^2P^o) + e$ (on the order of 10^{-6} cm^3/s).[48] According to the rate coefficient, it is estimated that the population distribution is given by the statistical weights if the electron density is higher than 1×10^{10} cm^{-3}, whereas the electron density in the present experimental condition is approximately 1×10^{11} cm^{-3}. The detailed kinetics of the $n = 2$ states of atomic hydrogen will be reported in a separate paper. We assume 500 K for the translational temperature of atomic hydrogen in Fig. 1, and the absorption spectrum is obtained by the superposition of the seven fine structure components with Doppler broadening corresponding to 500 K. We assume the unsaturated case, so that the amplitudes of the seven lines are proportional to the transition probabilities. The labels A-G in Fig 2(a) show the transitions indicated in Fig. 1.

The energy levels shown in Fig. 1 are degenerated. The degenerated states split into many levels in the presence of electric field, and as a result, we observe the change in the absorption spectrum. The wavelengths and the transition probabilities of fine-structure components with the Stark splitting can be calculated by solving the time-independent Schrödinger equation with the perturbation of the electric field.[49] An example of the Stark spectrum is shown in

Fig. 2(b), where we assume an electric field of 1 kV/cm and a translational temperature of 500 K. We assume that the electric field of the linearly polarized laser beam is parallel to the sheath electric field (the π polarization). As shown in Fig. 2(b), the absorption spectrum, which is obtained by the superposition of Doppler-broadened fine-structure components with the Stark splitting, is different from the field-free spectrum shown in Fig. 2(a).

The principle of the present method is to fit the theoretical spectrum with the absorption spectrum that is measured in the sheath. The physical values that are determined by the spectral fitting are the electric field strength and the translational temperature of atomic hydrogen. Figures 3(a) and 3(b) show the variations of the theoretical absorption spectra with the electric field and the translational temperature, respectively. The translational temperature is fixed at 500 K in Fig. 3(a), whereas the electric field is fixed at 0 V/cm in Fig. 3(b). Both the increases in the electric field and the translational temperature result in the broadening of the absorption spectrum, as shown in Fig. 3. We examine whether both the electric field and the translational temperature can be deduced from the absorption spectrum or not, and we evaluate the minimum electric field that can be detected by the present method.

3. Experiment

The experimental apparatus is schematically shown in Fig. 4. The plasma was produced in a cylindrical vacuum chamber with a diameter and a height of 26 cm. Pure hydrogen was introduced into the vacuum chamber after evacuating it below 4×10^{-6} Torr using a turbo molecular pump. The gas pressure was 47 mTorr. A one-turn rf antenna was inserted into the vacuum chamber, and it was connected to an rf power supply at 13.56 MHz via a matching circuit. The rf antenna was electrically insulated from the plasma by covering its surface with glass fibers. In this experiment, the rf power was pulse modulated at a frequency of 20 kHz. The instantaneous power and the duty factor were 1 kW and 50%, respectively. A planar electrode (5×15 cm^2) which was connected to a dc power supply was inserted into the vacuum chamber from the opposite side to the rf antenna. The distance between the planar electrode and the rf antenna was 5 cm.

The light source for absorption spectroscopy was a linearly-polarized, single-mode diode laser (New Focus TLB-6900). The oscillation wavelength of the diode laser was scanned around the Balmer-α line of atomic hydrogen. A mode hop free tuning range of 50 GHz was possible. The variation of the laser wavelength was monitored using a Fabry-Perot spectrum analyzer with a free spectral range of 1 GHz. The diode laser beam was injected into an optical fiber after passing through an optical isolator. The diode laser beam yielded from the

optical fiber was collimated, and it was injected into the plasma via an optical window. The diameter (FWHM) of the collimated laser beam was approximately 0.3 mm. The intensity of the laser beam was weak enough to avoid the saturation. The distance between the diode laser beam and the surface of the planar electrode was approximately 0.5 mm. The electric field of the linearly polarized laser beam was adjusted to be parallel (the π polarization) to the sheath electric field using a $\lambda/2$ plate. The laser beam transmitted through the plasma was detected using a photodiode. An interference filter which had the transmission at the wavelength of the Balmer-α line was placed in front of the photodiode to eliminate the optical emissions from the plasma. The electrical signal from the photodiode was connected to a lock-in amplifier to observe the synchronous component with the modulation frequency of the rf power. The lock-in amplifier was useful to obtain the absorption spectrum with a high signal-to-noise ratio.

4. Results and discussion

Figure 5 shows absorption spectra observed at three bias potentials of the planner electrode. The red curves with small noises are the experimental results, and the blue curves show the fittings with the theoretical spectra. The method of least squares was adopted to find the best fitting. As shown in the figures, we obtained fine fittings between the experimental and theoretical spectra by adjusting the electric field strength and the translational temperature. The electric field strength and the translational temperature, which were deduced by the spectral fitting, are summarized in Fig. 6 as a function of the electrode potential. The magnitudes of the error bars were evaluated on the basis of the ambiguity in the spectral fitting. We could not deduce the electric field at an electrode potential of 0 V since the ambiguity in the spectral fitting was too significant. As shown in the figure, we observed the monotonic increase in the electric field strength with the electrode potential. In contrast, we observed roughly constant translational temperature as a function of the electrode potential. This is a reasonable result since the heating of atomic hydrogen is not expected inside the nearly collisionless sheath at a pressure of 47 mTorr.

In a previous work, we reported the measurement of the electric field in the same plasma source by saturated absorption spectroscopy.[36] The electric field at a distance of 0.5 mm from the grounded electrode was approximately 25 V/cm. The electric field increased with the electrode potential monotonically, and they were $\sim$ 600, $\sim$ 850, and $\sim$ 1200 V/cm at electrode potentials of -40, -80, and -120 V, respectively, when the distance between the electrode surface and the measurement position was 0.4 mm. Considering the difference in the

measurement positions (0.4 and 0.5 mm from the electrode surface), the difference between the previous and present results is estimated to be within 40% when the electrode potential is deeper than -40 V. On the other hand, when the electrode potential was -20 V, the electric field measured by saturated absorption spectroscopy was ~ 250 V/cm at a distance of 0.4 mm from the electrode. This electric field is weaker than that determined by the present method at a distance of 0.5 mm, suggesting that the present method results in the overestimation of weak electric field.

This overestimation is related to the fact that the theoretical absorption spectrum does not change so much in weak electric field. Figure 7 represents the difference between the theoretical field-free spectrum and the theoretical spectra in electric fields. The vertical axis is given in the standard deviation. The amplitudes of the theoretical spectra are normalized so that the integral with respect to the frequency is equal to unity. As shown in the figure, the increase in the standard deviation is rather gentle at electric fields weaker than 200 V/cm, suggesting that the estimation of the electric field by the fitting between theoretical and experimental spectra may contain a large error. Actually, the standard deviation between the theoretical field-free spectrum and the experimental spectrum observed at an electrode potential of 0 V is 1.6×10^{-12} Hz^{-1}. This is the reason for the fact that the estimation of the electric field is impossible at an electrode potential of 0 V and for the large error bar shown in Fig. 6(a) at an electrode potential of -20 V. Therefore, considering the magnitude of the ambiguity in the spectral fitting and the standard deviation shown in Fig. 7, it is evaluated that the minimum electric field that can be determined by the present method is approximately 350 V/cm. This detection limit is comparable to the detection limits obtained by optogalvanic spectroscopy[24,25] and laser-induced collisional fluorescence spectroscopy,[26,27] where pulsed dye lasers are used for exciting metastable states of helium and argon to Rydberg states with principal quantum numbers of $n = 7 - 14$.

5. Conclusions

We examined the applicability of the Doppler-broadened absorption spectrum of the hydrogen Balmer-α line to the estimation of the sheath electric field in plasma. The Doppler-broadened absorption spectrum was measured by standard laser absorption spectroscopy. The conclusion is that the method works in electric fields higher than ~ 350 V/cm, when the translational temperature of atomic hydrogen is 400-500 K. This sensitivity is worse than those of laser-induced fluorescence-dip spectroscopy[28–34] and saturated absorption spectroscopy,[35,36] but it is comparable to optogalvanic spectroscopy[24,25] and laser-induced collisional fluores-

cence spectroscopy.[26,27] The light source in the present method is a diode laser, and the optical configuration is simple (the standard laser absorption spectroscopy). Therefore, we believe that the present method is useful in many experiments where an easy-to-use method for measuring the sheath electric fields is demanded.

Acknowledgments

The authors are grateful to Motoshi Goto for giving them the permission to use the numerical code for calculating the Stark effect of the hydrogen Balmer-α line.

References

1) R. N. Franklin, J. Phys. D: Appl. Phys. **36**, R309 (2003).
2) N. Hershkowitz, Phys. Plasmas **12**, 055502 (2005).
3) M. A. Lieberman and A. J. Lichtenberg, *Principles of Plasma Discharges and Materials Processing, 2nd ed.* (Wiley-Interscience, Hoboken, 2005).
4) T. E. Sheridan and M. J. Goeckner, J. Appl. Phys. **77**, 4967 (1995).
5) H.-B. Valentinia, Phys. Plasmas **3**, 1459 (1996).
6) K. U. Riemann and P. Meyer, Phys. Plasmas **3**, 4751 (1996).
7) H.-B. Valentinia, Phys. Plasmas **3**, 4754 (1996).
8) M. S. Benilov, Phys. Rev. E **77**, 036408 (2008).
9) R. N. Franklin and J, Snell, J. Phys. D: Appl. Phys. **31**, 2532 (1998).
10) A. Kono, J. Phys. D: Appl. Phys. **34**, 1083 (2001).
11) A. Kono, J. Phys. D: Appl. Phys. **36**, 465 (2003).
12) B. M. Annaratone, T. Antonova, H. M. Thomas, and G. E. Morfill, Phys. Rev. Lett. **93**, 185001 (2004).
13) K. Takizawa, A. Kono, and K. Sasaki, Appl. Phys. Lett. **90**, 011503 (2007).
14) G. D. Severn, X. Wang, E. Ko, and N. Hershkowitz, Phys. Rev. Lett. **90**, 145001 (2003).
15) D. Lee, G. Severn, L. Oksuz, and N. Hershkowitz, J. Phys. D: Appl. Phys. **39**, 5230 (2006).
16) S. D. Baalrud, C. C. Hegna, and J. D. Callen, Phys. Rev. Lett. **103**, 205002 (2009).
17) V. Godyak and N. Sternberg, Phys. Plasmas **9**, 4427 (2002).
18) V. Godyak and N. Sternberg, Phys. Plasmas **10**, 44587 (2003).
19) N. Sternberg and V.Godyak, IEEE Tans. Plasma Sci. **31**, 665 (2003).
20) K-U. Riemann, J. Phys. D: Appl. Phys **36**, 2811 (2003).
21) R.N. Franklin, J. Phys. D: Appl. Phys **37**, 1342 (2004).
22) A. Kono, J. Phys. D: Appl. Phys. **37**, 1945 (2004).
23) L. Oksuz and N. Hershkowitz, Plasma Sources Sci. Technol. **14**, 201 (2005).
24) D. K. Doughty and J. E. Lawler, Appl. Phys. Lett. **45**, 611 (1984).
25) V. P. Gavrilenko, H. J. Kim, T. Ikutake, J. B. Kim, Y. W. Choi, M. D. Bowden, and K. Muraoka, Phys. Rev. E **62**, 7201 (2000).
26) K. E. Greenberg and G. A. Hebner, Appl. Phys. Lett. **63**, 3282 (1993).
27) Y. W. Choi, M. D. Bowden, and K. Muraoka, Appl. Phys. Lett. **69**, 1361 (1996).
28) U. Czarnetzki, D. Luggenhölscher, and H. F. Döbele, Phys. Rev. Lett. **81**, 4592 (1998).

29) K. Takizawa, K. Sasaki, and K. Kadota, Jpn. J. Appl. Phys. **41**, L1285 (2002).
30) K. Takizawa, K. Sasaki, and A. Kono, Appl. Phys. Lett. **84**, 185 (2004).
31) E. V. Barnat and G. A. Hebner, Appl. Phys. Lett. **85**, 3393 (2004).
32) K. Takizawa, A. Kono, and K. Sasaki K, Jpn. J. Appl. Phys. **46**, 6822 (2007).
33) E. Wagenaars, M. D. Bowden, and G. M. W. Kroesen, Phys. Rev. Lett. **98**, 075002 (2007).
34) T. Kampschulte, J. Schulze, D. Luggenhölscher, M. D. Bowden, and U. Czarnetzki, New. J. Phys. **9**, 18 (2007).
35) S. Nishiyama, K. Katayama, H. Nakano, M. Goto, and K. Sasaki, Appl. Phys. Express **10**, 036101 (2017).
36) S. Nishiyama, H. Nakano, M. Goto, and K. Sasaki, J. Phys. D: Appl. Phys. **50**, 234003 (2017).
37) B. N. Ganguly and A. Garscadden, J. Appl. Phys. **70**, 621 (1991).
38) R. Casini and P. Foukal, Solar Phys. **163**, 65 (1996).
39) I. R. Videnović, N. Konjević, and M.M. Kuraica, Spectrochim. Acta Part B **51**, 1707 (1996).
40) N. Cvetanović, M. M. Kuraica, and N. Konjević, J. Appl. Phys. **97**, 033302 (2005).
41) H. W. Janus, J. Phys. D: Appl. Phys. **40**, 3608 (2007).
42) N. Cvetanović, S. S. Ivković, B. M. Obradović, and M. M. Kuraica, Eur. Phys. J. D **71**, 317 (2017).
43) J. Vetterhöffer, A. Campargue, M. Chenevier, and F. Stoeckel, Diam. Relat. Mater. **2**, 481 (1993).
44) A. Rousseau, E. Teboul, and N Sadeghi, Plasma Sources Sci. Technol. **13**, 166 (2004).
45) M. Aramaki, Y. Okumura, M. Goto, S. Muto, S. Morita, and K. Sasaki, Jpn. J. Appl. Phys. **44**, 6759 (2005).
46) W. E. N. van Harskamp, C. M. Brouwer, D. C. Schram, M. C. M. van de Sanden, and R. Engeln, Plasma Sources Sci. Technol. **21**, 024009 (2012).
47) C. M. Samuell and C. S. Corr, Plasma Sources Sci. Technol. **24**, 045003 (2015).
48) R. K. Janev, W. D. Langer, K. Evans, Jr., and D. E. Post, Jr., *Elementary Processes in Hydrogen-Helium Plasmas* (Springer-Verlag, Berlin, 1987).
49) T. Fujimoto and A. Iwamae (Eds.), *Plasma Polarization Spectroscopy* (Springer, Berlin, 2008)

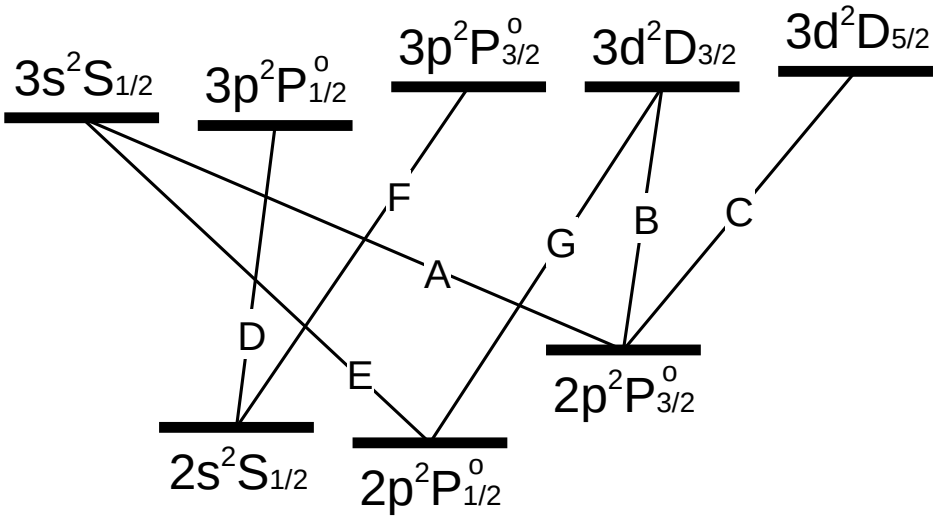

Fig. 1. Energy level diagram of atomic hydrogen relevant to the Balmer-α line.

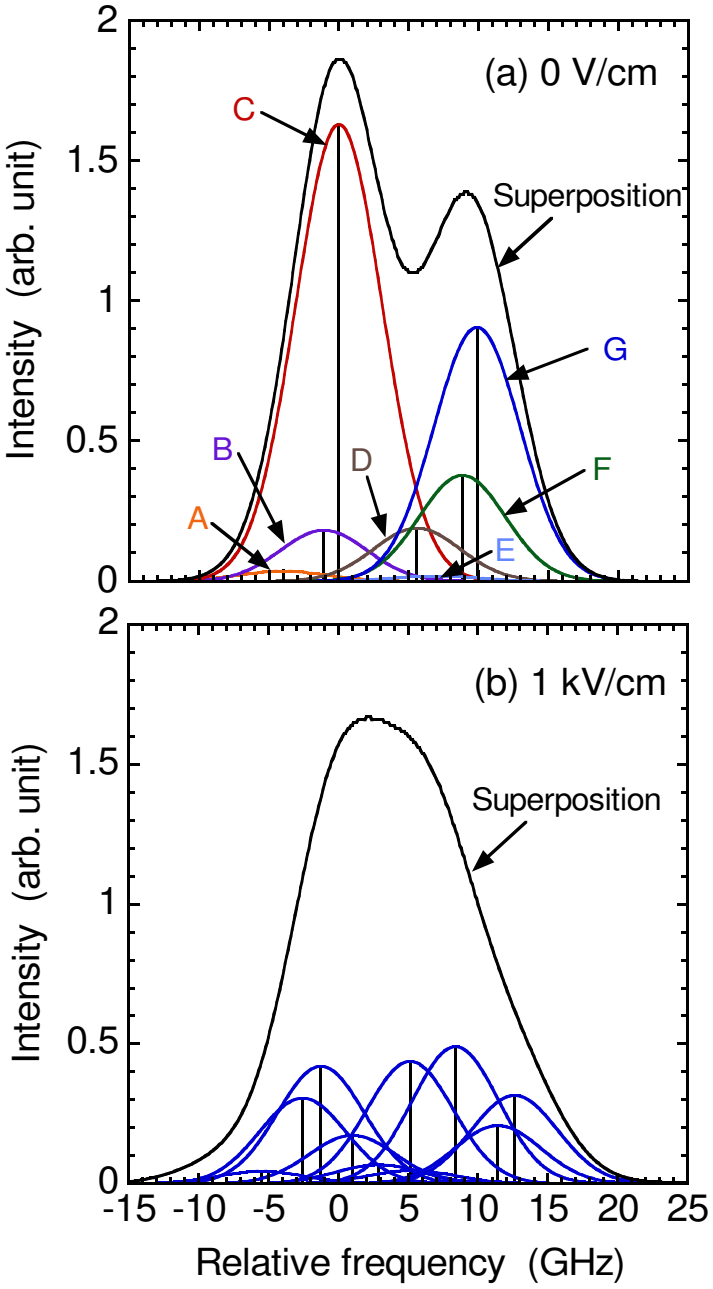

Fig. 2. Theoretical absorption spectra (a) in field-free condition and (b) in electric field of 1 kV/cm. The fine structure components (a) without and (b) with the Stark splitting are also illustrated. The Doppler broadening corresponding to 500 K is assumed for each fine structure component. The electric field of linearly polarized laser beam is assumed to be parallel to the sheath electric field. The labels A-G in (a) correspond to the transitions shown in Fig. 1.

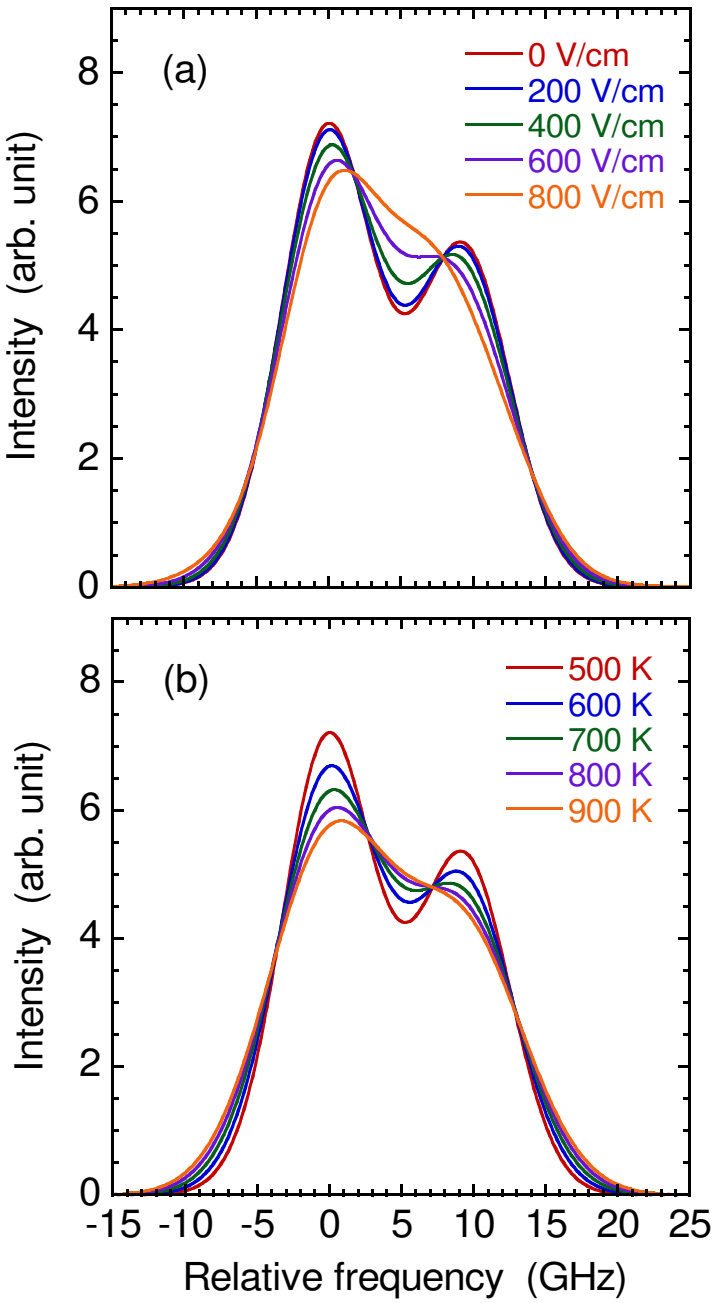

Fig. 3. Theoretical absorption spectra at (a) various electric fields and (b) various translational temperatures. The translational temperature is fixed at 500 K in (a), whereas the electric field is fixed at 0 V/cm in (b).

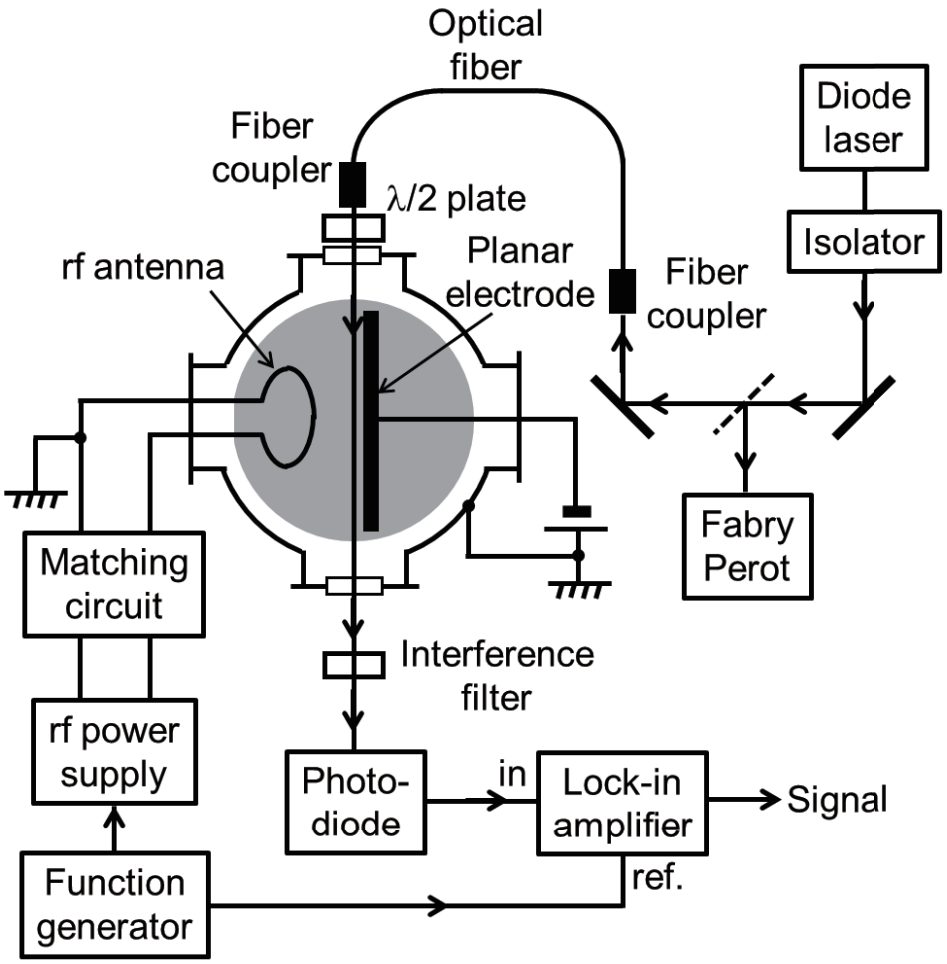

Fig. 4. Schematic of experimental apparatus.

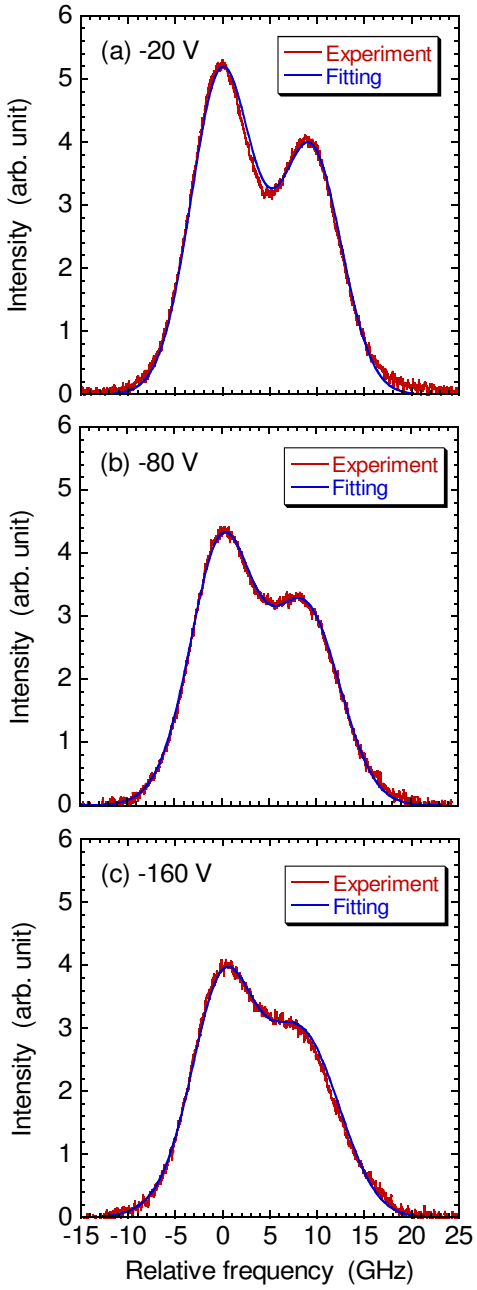

Fig. 5. Absorption spectra observed at electrode potentials of (a) -20 V, (b) -80 V, and (c) -160 V. The theoretical spectra which are fitted with experimental spectra are also shown.

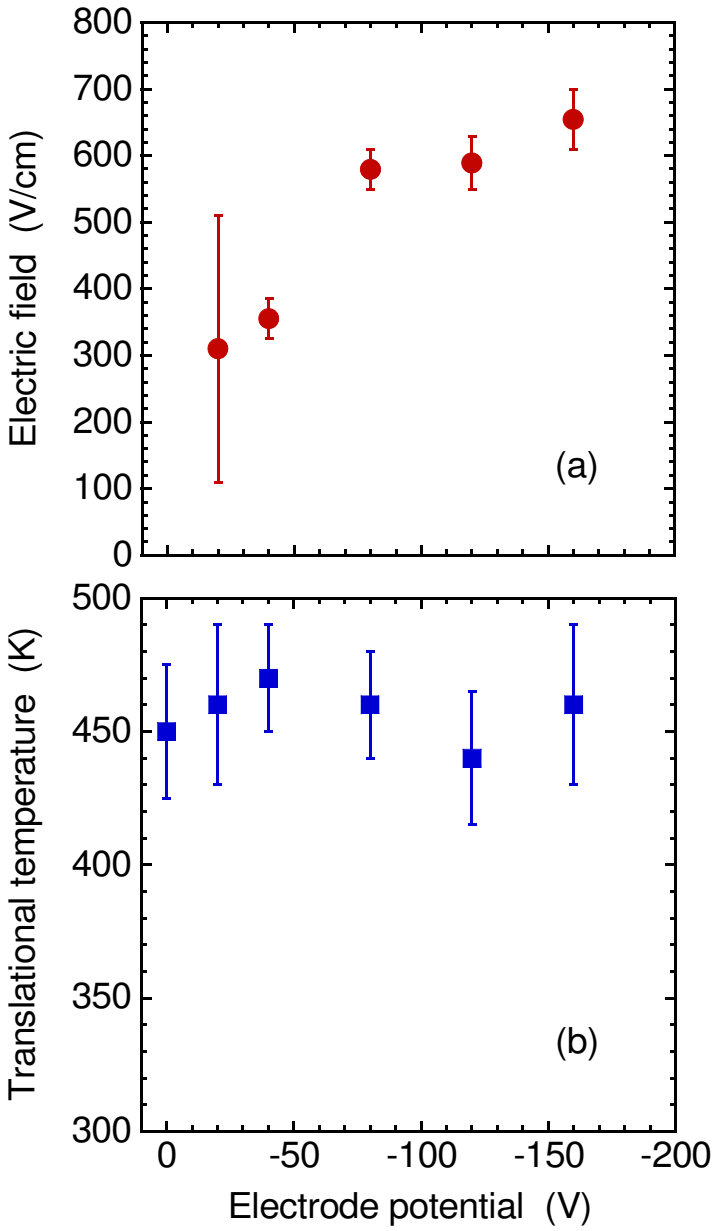

Fig. 6. (a) Electric field strength and (b) translational temperature, which are deduced by the fitting between experimental and theoretical spectra, as a function of the electrode potential.

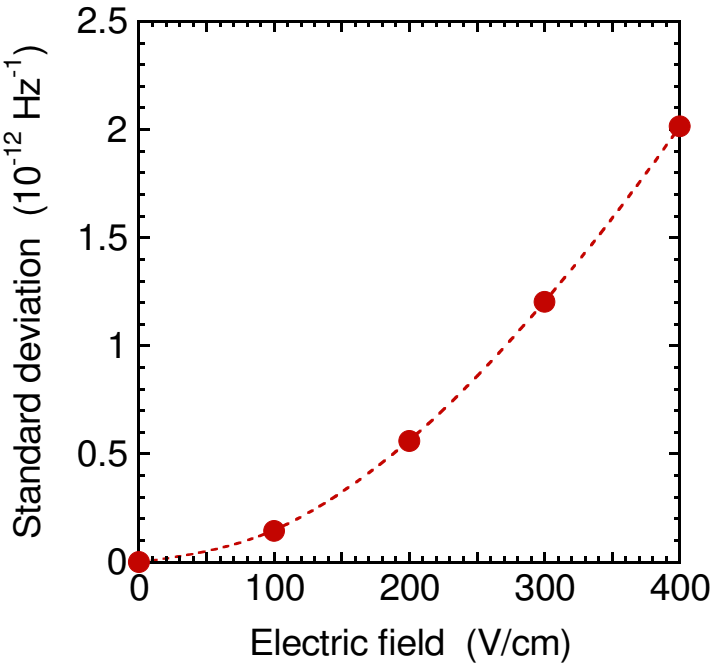

Fig. 7. Difference (given in standard deviation) between theoretical field-free spectrum and spectrum in electric fields.